NASA / TM—1998-206962

Friction and Wear Properties of a-DLC-Based Functionally Gradient Nanocomposite Coatings

Kazuhisa Miyoshi and Kenneth W. Street
Lewis Research Center, Cleveland, Ohio

Jeffrey S. Zabinski, Jeffrey H. Sanders, and Andrey A. Voevodin
Air Force Research Laboratory, Wright-Patterson Air Force Base, Ohio

March 1998

The NASA STI Program Office . . . in Profile

Since its founding, NASA has been dedicated to the advancement of aeronautics and space science. The NASA Scientific and Technical Information (STI) Program Office plays a key part in helping NASA maintain this important role.

The NASA STI Program Office is operated by Langley Research Center, the Lead Center for NASA's scientific and technical information. The NASA STI Program Office provides access to the NASA STI Database, the largest collection of aeronautical and space science STI in the world. The Program Office is also NASA's institutional mechanism for disseminating the results of its research and development activities. These results are published by NASA in the NASA STI Report Series, which includes the following report types:

- TECHNICAL PUBLICATION. Reports of completed research or a major significant phase of research that present the results of NASA programs and include extensive data or theoretical analysis. Includes compilations of significant scientific and technical data and information deemed to be of continuing reference value. NASA's counterpart of peer-reviewed formal professional papers but has less stringent limitations on manuscript length and extent of graphic presentations.

- TECHNICAL MEMORANDUM. Scientific and technical findings that are preliminary or of specialized interest, e.g., quick release reports, working papers, and bibliographies that contain minimal annotation. Does not contain extensive analysis.

- CONTRACTOR REPORT. Scientific and technical findings by NASA-sponsored contractors and grantees.

- CONFERENCE PUBLICATION. Collected papers from scientific and technical conferences, symposia, seminars, or other meetings sponsored or cosponsored by NASA.

- SPECIAL PUBLICATION. Scientific, technical, or historical information from NASA programs, projects, and missions, often concerned with subjects having substantial public interest.

- TECHNICAL TRANSLATION. English-language translations of foreign scientific and technical material pertinent to NASA's mission.

Specialized services that complement the STI Program Office's diverse offerings include creating custom thesauri, building customized data bases, organizing and publishing research results . . . even providing videos.

For more information about the NASA STI Program Office, see the following:

- Access the NASA STI Program Home Page at ***http://www.sti.nasa.gov***

- E-mail your question via the Internet to help@sti.nasa.gov

- Fax your question to the NASA Access Help Desk at (301) 621-0134

- Telephone the NASA Access Help Desk at (301) 621-0390

- Write to:
  NASA Access Help Desk
  NASA Center for AeroSpace Information
  800 Elkridge Landing Road
  Linthicum Heights, MD 21090-2934

NASA / TM—1998-206962

Friction and Wear Properties of a-DLC-Based Functionally Gradient Nanocomposite Coatings

Kazuhisa Miyoshi and Kenneth W. Street
Lewis Research Center, Cleveland, Ohio

Jeffrey S. Zabinski, Jeffrey H. Sanders, and Andrey A. Voevodin
Air Force Research Laboratory, Wright-Patterson Air Force Base, Ohio

National Aeronautics and
Space Administration

Lewis Research Center

March 1998

Available from

NASA Center for Aerospace Information
800 Elkridge Landing Road
Linthicum Heights, MD 21090-2934
Price Code: A03

National Technical Information Service
5287 Port Royal Road
Springfield, VA 22100
Price Code: A03

FRICTION AND WEAR PROPERTIES OF a-DLC-BASED FUNCTIONALLY GRADIENT NANOCOMPOSITE COATINGS

Kazuhisa Miyoshi and Kenneth W. Street
National Aeronautics and Space Administration
Lewis Research Center
Cleveland, Ohio 44135

Jeffrey S. Zabinski, Jeffrey H. Sanders, and Andrey A. Voevodin
Air Force Research Laboratory
Wright-Patterson Air Force Base, Ohio 45433–7750

SUMMARY

An investigation was conducted to examine the friction and wear behavior of an amorphous diamondlike carbon (a-DLC or a-C) functionally gradient nanocomposite coating in sliding contact with a 6-mm-diameter silicon nitride ball and a 6-mm-diameter 440C stainless steel ball in ultrahigh vacuum and in humid air. The nanocomposite coatings, consisting of an a-DLC top layer and a gradient Ti-Ti_xC_y-DLC underlayer, were produced by the hybrid technique of magnetron sputtering and pulsed-laser deposition on 440C stainless steel substrates.

The resultant coatings were characterized by Raman spectroscopy, scanning electron microscopy, energy-dispersive x-ray spectroscopy, and surface profilometry. All sliding friction experiments were conducted with a load of 0.98 N (100 g), average Hertzian contact pressures of 0.6 GPa with the 440C stainless steel balls and 0.8 GPa with the silicon nitride balls, and 120 revolutions per minute. The sliding velocity ranged from 31 to 107 mm/s because of the range of wear track radii involved in the experiments. The experiment was conducted at room temperature in two environments: ultrahigh vacuum (vacuum pressure, 7×10^{-7} to 2×10^{-6} Pa) and humid air (relative humidity, about 50%).

A marked difference in friction and wear resulted from the environmental conditions and the combination of materials. The humid air caused mild wear with burnishing in the a-DLC top layer; the ultrahigh vacuum caused relatively severe wear with brittle fracture in both the a-DLC top layer and the Ti-Ti_xC_y-DLC underlayer. The humid air environment provided a low coefficient of friction, a low wear rate for the a-DLC top layer, and a low wear rate for the 440C stainless steel ball (counterpart material). In ultrahigh vacuum the materials pair of a-DLC coated substrate and 440C stainless steel ball was superior in wear resistance to the pair of a-DLC and silicon nitride ball, although both pairs had high coefficients of friction. The wear rate was low in both environments for both the a-DLC coated substrate and the 440C stainless steel ball. Changes in the bonding state and structure of the a-DLC layer were observed during the sliding friction process. The amorphous, disordered nondiamond form of carbon was produced during sliding contact.

INTRODUCTION

The nature of the substrate and its predeposition treatment play a major role in determining the load-carrying capacity and wear resistance of diamondlike carbon (DLC) coatings in tribological applications. Especially when the DLC coatings are applied to relatively soft substrates, such as steels, the brittle nature and high internal compressive stresses (1 to 2 GPa) of DLC may limit the applications to light loads. In other words, the maximum load that a sliding or rolling system can support without failure or wear exceeding the design limits for the particular application is low. Therefore, synergetic characteristics of a-DLC, such as bending strength, shear strength, elasticity, and hardness, as well as adhesion of DLC to its substrate in DLC-substrate systems, must be improved through methods such as multilayer DLC coatings (refs. 1 to 8) and compositional modification of DLC (refs. 9 to 14).

In a previous study conducted by Voevodin, Walck, and Zabinski (ref. 1), several design concepts, including Ti-Ti_xC_y-DLC functionally gradient nanocomposite coatings, were developed to increase the fracture toughness of DLC-based coatings while preserving the superhardness (60 to 70 GPa) of DLC. The study demonstrated how the potential of superhard DLC coatings for wear protection can be multiplied by the development of functionally gradient nanocomposite designs.

This present investigation was conducted to examine the friction and wear properties of amorphous DLC-based functionally gradient nanocomposite (a-DLC/Ti-Ti_xC_y-DLC) coatings in ultrahigh vacuum and in humid air at a relative humidity of approximately 50%. The a-DLC/Ti-Ti_xC_y-DLC functionally gradient nanocomposite coatings consisting of an a-DLC top layer and a gradient Ti-Ti_xC_y-DLC underlayer were produced by the hybrid of magnetron sputtering and pulsed-laser deposition on 440C stainless steel substrates. Unidirectional ball-on-disk sliding friction experiments were conducted with 440C stainless steel balls or silicon nitride (Si_3N_4) balls in sliding contact with a-DLC/Ti-Ti_xC_y-DLC coatings at room temperature in ultrahigh vacuum and in humid air. The resultant a-DLC-based functionally gradient nanocomposite coatings and their wear surfaces were characterized by Raman spectroscopy, scanning electron microscopy (SEM), energy-dispersive x-ray spectroscopy (EDX), and surface profilometry. Raman spectroscopy was used to characterize carbon bonding and its chemical structure. SEM and EDX were used to determine the morphology and elemental composition of wear surfaces and wear debris. The sampling depth of EDX for elemental information ranges between 0.5 to 1 μm in this investigation. Surface profilometry was used to determine the surface morphology, roughness, and wear of the coatings.

MATERIALS

Figure 1 is a schematic diagram of the a-DLC/ Ti-Ti_xC_y-DLC functionally gradient nanocomposite coating consisting of the a-DLC top layer on the gradient Ti-Ti_xC_y-DLC underlayer. The composition and properties of the coatings are also shown in the figure. Reference 15 provides detailed analyses of the gradations of compositional, structural, and mechanical properties in the gradient coating. In the coating the composition varied from titanium to a-DLC through an intermediate Ti_xC_y ceramic region, and the hardness generally increased gradually from the 440C stainless steel substrate to the a-DLC, preventing sharp changes in chemistry, structure, and mechanical properties.

The a-DLC/ Ti-Ti_xC_y-DLC multilayer coatings were prepared with a hybrid technology called magnetron-sputter-assisted, pulsed-laser deposition (MSPLD), described in reference 16. Fluxes of energetic carbon from pulsed-laser deposition and titanium atoms from magnetron sputtering were intersected on the substrate surface. The individual fluxes were controlled independently to provide a preprogrammed variation of the composition and structure across the coating thickness. Laser beam scanning and specimen positioning ensured a uniform coating without compositional variations in directions parallel to the substrate surface. All depositions were performed with substrate temperatures of 100 °C. The substrates were 440C stainless steel disks (3 mm thick, 25 mm diameter) heat treated to the microhardness of 7 to 8 GPa and polished to below 0.1-μm centerline-average roughness. They were etched with 1 keV of argon ions for 30 min prior to deposition. The functionally gradient nanocomposite coating comprised an approximately 0.5-μm-thick DLC layer on a 0.45-μm-thick gradient Ti-Ti_xC_y-DLC underlayer.

Six specimens of the a-DLC/Ti-Ti_xC_y-DLC functionally gradient nanocomposite coatings deposited on 440C stainless steel disk substrates were used in this investigation. Their surfaces were smooth and their centerline-average roughness R_a, meas-ured using a cutoff of 1 mm, was 19 nm with a standard deviation of 5 nm. Figure 2 presents a typical EDX spectrum and Raman spectrum of the a-DLC/ Ti-Ti_xC_y-DLC functionally gradient nanocomposite coating. The EDX spectrum primarily contains the elements of the a-DLC/ Ti-Ti_xC_y-DLC functionally gradient nanocomposite coating and the 440C stainless steel substrate, particularly a high concentration of carbon and titanium. The Raman spectrum indicates the presence of amorphous nondiamond carbon in the a-DLC top layer, but the characteristic sp^3-bonded diamond peak is absent. The spectrum shows that sp^2-bonded graphitic amorphous carbon was prevalent in the a-DLC.

The 6-mm-diameter 440C stainless steel balls (grade number, 10) and the 6-mm-diameter silicon nitride balls (grade number, 5) were also smooth; the surface roughnesses R_a were 0.025 μm and 0.02 μm or less, respectively.

EXPERIMENT

Unidirectional ball-on-disk sliding friction experiments were conducted in ultrahigh vacuum at a vacuum pressure of 7×10^{-7} to 2×10^{-6} Pa and in humid air (relative humidity approx. 50%) at room temperature. All experiments were conducted with a load of 0.98 N (100 g) at a constant 120 revolutions per minute (the sliding velocity from 31 to 107 mm/s because of the wear track radii involved in the experiments). The friction-and-wear apparatus used in the investigation was mounted in a vacuum chamber (fig. 3). The apparatus can measure friction both in vacuum and in humid air during sliding. Wear can be quantified by measuring the size of wear scar and wear track on the

specimens after the wear experiment. All experiments were conducted with 6-mm-diameter 440C stainless steel balls and 6-mm-diameter silicon nitride balls in sliding contact with a-DLC/Ti-Ti_xC_y-DLC functionally gradient nanocomposite coatings deposited on 440C stainless steel substrate disks. The mean Hertzian contact pressures of the a-DLC/Ti-Ti_xC_y-DLC functionally gradient nanocomposite coating in contact with the 440C stainless steel and silicon nitride balls were approximately 0.6 GPa and 0.8 GPa, respectively. The friction force was continuously monitored during the friction experiments. Coating wear volumes were obtained by measuring the average cross-sectional area, determined from stylus tracings, across the wear tracks at a minimum of eight locations in each wear track. Then, the average cross-sectional area of the wear track was multiplied by the wear track length. The wear rate, known as the dimensional wear coefficient, is defined as the volume of material removed at a unit load and in a unit sliding distance expressed as cubic millimeters per newton•meter.

RESULTS AND DISCUSSION

a-DLC Coating in Sliding Contact With Si_3N_4 Ball in Ultrahigh Vacuum

Friction behavior.—Figure 4 presents a typical friction trace obtained in ultrahigh vacuum for a-DLC/Ti-Ti_xC_y-DLC functionally gradient nanocomposite coatings in sliding contact with silicon nitride balls as a function of the number of passes. The mean steady-state coefficient of friction was relatively high, approximately 0.6 from 200 to 800 or 900 passes. From 800 or 900 passes to 5000 passes the coefficient of friction decreased to approximately 0.56. After 5000 passes the coefficient of friction gradually increased to 0.9 at 10 000 passes.

Coating wear behavior.—Figures 5 and 6 show SEM photomicrographs and EDX spectra, respectively, of the worn surfaces of a-DLC/Ti-Ti_xC_y-DLC functionally gradient nanocomposite coatings in sliding contact with Si_3N_4 balls after 300, 1000, and 10 000 passes in ultrahigh vacuum. After 300 passes (fig. 5(a)) the worn surface was relatively smooth, and EDX analysis indicated that it contained the elements of the a-DLC/Ti-Ti_xC_y-DLC coating. After 1000 passes (fig. 5(b)) the worn surface was relatively smooth in the upper and lower regions of the wear track, indicating that the a-DLC top layer was still present. The center region of the wear track, however, revealed a rougher surface, indicating delamination of the a-DLC top layer and exposure of the Ti-Ti_xC_y underlayer. Closer SEM examination at high magnification of the boundary between the smooth and rough wear track surfaces showed fracturing and fragmentation of the a-DLC top layer and exposure of the underlayer in the rougher center region. EDX analysis of the wear-damaged center region (fig. 6(b)) indicated that it contained less carbon than it had after 300 passes. After 10 000 passes (fig. 5(c)) the a-DLC top layer was not present on the worn surface. Closer SEM examination at high magnification showed carbon wear debris particles locally present on the wear track. EDX analysis of the center region after 10 000 passes (fig. 6(c)) indicated not only less carbon but also less titanium on the 440C stainless steel disk substrate than after 300 and 1000 passes.

Figure 7 presents Raman spectra of the as-deposited surface of an a-DLC/Ti-Ti_xC_y-DLC functionally gradient nanocomposite coating and the worn surface after 10 000 passes. The Raman spectrum taken from the worn surface contained much less carbon than the as-received surface, consistent with the EDX result shown in figure 6(c).

Silicon nitride ball wear behavior.—Figure 8 presents SEM photomicrographs of the wear scars on silicon nitride balls after 300, 1000, and 10 000 sliding passes against a-DLC/Ti-Ti_xC_y-DLC functionally gradient nanocomposite coatings in ultrahigh vacuum. The wear scars produced after 300 and 1000 passes (figs. 8(a) and (b)) were relatively smooth, although the wear scar observed at high magnification after 1000 passes contained relatively greater wear damage and microfracturing than after 300 passes. The wear scar produced after 10 000 passes (fig. 8(c)) had severe wear damage and transferred materials, and closer SEM examination at high magnification clearly showed transferred patches of materials from the a-DLC/Ti-Ti_xC_y-DLC coating.

As shown in figure 9, EDX spectra taken at the center of the ball wear scars indicated that all contained elements, such as carbon and titanium, from the counterpart material (a-DLC/Ti-Ti_xC_y-DLC). The carbon and titanium concentrations on the wear scar surface increased with an increase in the number of passes during sliding.

a-DLC Coating in Sliding Contact With Steel Ball in Ultrahigh Vacuum and in Humid Air

Friction behavior.—Figure 10 presents typical friction traces obtained in ultrahigh vacuum and in humid air for a-DLC/Ti-Ti_xC_y-DLC functionally gradient nanocomposite coatings in sliding contact with 440C stainless steel

balls as a function of the number of passes to 10 000 passes. The friction traces show that the coefficient of friction strongly depended on the environment. The mean coefficients of friction obtained in ultrahigh vacuum were higher than those obtained in humid air by a factor of 3 to 10. Also, the irregularities in the friction traces were much higher in ultrahigh vacuum than in humid air.

Coating wear behavior in ultrahigh vacuum.—Figures 11 and 12 present SEM photomicrographs and EDX spectra, respectively, of the worn surfaces of a-DLC/Ti-Ti_xC_y-DLC functionally gradient nanocomposite coatings in sliding contact with 440C stainless steel balls after 3000, 6000, and 10 000 passes in ultrahigh vacuum. After 3000 passes (fig. 11(a)) the relatively smooth surfaces in the upper and lower regions of the wear track indicated that the a-DLC top layer was still present. The rougher surface in the center of the wear track, however, indicated delamination of the a-DLC top layer and exposure of the Ti-Ti_xC_y underlayer. Closer SEM examination at high magnification of the boundary region between the smooth and rough wear track surfaces (fig. 11(a)) showed that the a-DLC top layer in the rougher wear track region had fractured and fragmented, exposing the underlayer. EDX analysis of the wear-damaged area at the center of the wear track after 3000 passes (fig. 12(a)) revealed that it contained much less carbon than the unworn surface area. After 6000 passes (fig. 11(b)) the worn surface indicated removal of the a-DLC top layer and exposure of the Ti-Ti_xC_y underlayer. Closer SEM examination at high magnification of the upper edge of the wear track (fig. 11(b)) showed that the a-DLC top layer and the Ti-Ti_xC_y underlayer were locally removed from the 440C stainless steel substrate. EDX analysis of the center of the wear track after 6000 passes (fig. 12(b)) revealed that it contained less carbon and titanium than either the worn surface after 3000 passes or the unworn surface area. After 10 000 passes (fig. 11(c)) the worn surface indicated substantial wear damage to the functionally gradient nanocomposite coating. The a-DLC top layer was completely removed from the wear track. Closer SEM examination of the wear track at high magnification (fig. 11(c)) showed the worn and exposed surface of the Ti-Ti_xC_y underlayer. EDX analysis of the center of the wear track after 10 000 passes (fig. 12(c)) revealed that it contained less carbon and titanium than either the worn surfaces after 3000 and 6000 passes or the unworn surface area.

Wear behavior of 440C stainless steel ball in ultrahigh vacuum.—Figure 13 presents SEM photomicrographs and an EDX spectrum of the wear scar on a 440C stainless steel ball after 10 000 sliding passes against the a-DLC/Ti-Ti_xC_y-DLC functionally gradient nanocomposite coating in ultrahigh vacuum. The SEM photomicrograph taken at a low magnification shows that the wear scar was generally smooth but partially covered by smeared patches of wear debris. Smeared, agglomerated wear debris accumulated around the contact border, particularly on the rear end of the wear scar. Closer SEM examination at a higher magnification of the contact border at the rear end of the wear scar showed smearing, fracturing, and fragmentation of wear debris. The center of the wear track revealed a rougher surface, indicating micro-scratches and smeared patches of wear debris with cracks. An EDX spectrum taken at the center of the wear scar revealed that it contained elements, such as carbon and titanium, from the counterpart material (the a-DLC/Ti-Ti_xC_y-DLC functionally gradient nanocomposite coating). This evidence indicates that the wear debris patches on the wear scar contained transferred materials.

Coating wear behavior in humid air.—Figure 14 shows mean coefficients of friction as a function of the number of passes as well as SEM photomicrographs and an EDX spectrum of the wear track after 550 000 passes in humid air. The worn surface after 550 000 passes was relatively smooth in the wear track and revealed mild wear of the a-DLC/Ti-Ti_xC_y-DLC functionally gradient nanocomposite coating. Although the height of the carbon peak in the EDX spectrum decreased owing to wear of the a-DLC top layer, the a-DLC top layer was still present even after 550 000 passes in humid air.

Wear behavior of 440C stainless steel ball in humid air.—Figure 15 presents SEM photomicrographs and an EDX spectrum of the wear scar on a 440C stainless steel ball after 550 000 sliding passes against the a-DLC/Ti-Ti_xC_y-DLC functionally gradient nanocomposite coating in humid air. The SEM photomicrograph taken at a low magnification shows smeared patches and fragmentation of wear debris in and around the wear scar. Closer SEM examination at a high magnification of the center of the wear scar revealed smeared, agglomerated wear debris accumulated on and attached to the wear scar. An EDX spectrum taken at the center of the wear scar revealed that it contained elements from the 440C stainless steel ball and also elements, such as titanium and carbon, from the counterpart material (the a-DLC/Ti-Ti_xC_y-DLC functionally gradient nanocomposite coating). Comparing figure 15 with figure 14 shows that the wear debris patches on the wear scar produced in humid air contained much less transferred wear debris materials than those on the wear scar produced in ultrahigh vacuum.

The humid air environment caused mild wear with burnishing in the a-DLC top layer, whereas the ultrahigh vacuum environment caused relatively severe wear with brittle fracture in the a-DLC top layer and the Ti-Ti_xC_y-DLC underlayer.

Comparison of Steady-State Coefficients of Friction, Wear Lives, and Wear Rates

Table I summarizes the steady-state coefficients of friction, coating wear rates, and ball wear rates for the pair of a-DLC/Ti-Ti_xC_y-DLC functionally gradient nanocomposite coating and silicon nitride ball and for the pair of a-DLC/Ti-Ti_xC_y-DLC functionally gradient nanocomposite coating and 440C stainless steel ball in ultrahigh vacuum and in humid air. The data presented in the table indicate the marked difference in friction and wear resulting from the environmental conditions and combinations of materials.

Ultrahigh vacuum environment.—With the materials pair of a-DLC/Ti-Ti_xC_y-DLC and silicon nitride ball in ultrahigh vacuum, the a-DLC top layer started to delaminate at 800 to 900 passes. This number is the critical number of passes to delaminate the a-DLC top layer and corresponds to the wear life of the a-DLC top layer sliding against the silicon nitride ball. Up to 800 to 900 passes the steady-state coefficient of friction was approximately 0.60, which was high; and the wear rates of both the a-DLC layer and the silicon nitride ball were on the order of 10^{-6} $mm^3/N•m$. After 800 passes the coating wear rate and the coefficient of friction decreased, but the ball wear rate was similar to that before 800 passes. These sliding conditions continued to 5000 passes. After 5000 passes the a-DLC top layer was almost completely removed from the wear track, and sliding contacts between the Ti-Ti_xC_y underlayer and the silicon nitride ball occurred. After 5000 passes the coating wear rate and the coefficient of friction markedly increased, but the ball wear rate decreased.

With the materials pair of a-DLC/Ti-Ti_xC_y-DLC and 440C stainless steel ball in ultrahigh vacuum, the a-DLC layer started to delaminate at 1100 to 1200 passes. This number is the critical number of passes to delaminate the a-DLC top layer and corresponds to the wear life of the a-DLC top layer sliding against the 440C stainless steel ball. Up to 1100 to 1200 passes the steady-state coefficient of friction was approximately 0.56, which was high; the wear rate of the a-DLC layer was on the order of 10^{-6} $mm^3/N•m$; and the wear rate of the 440C stainless steel ball was on the order of 10^{-7} $mm^3/N•m$. The a-DLC layer provided an acceptable level of wear for the materials pair of a-DLC and 440C stainless steel. After 1000 to 1200 passes the coating wear rate and the coefficient of friction increased. After 4400 to 6500 passes the a-DLC top layer was almost completely removed from the wear track, and sliding contacts between the Ti-Ti_xC_y underlayer and the 440C stainless steel ball occurred. After 4400 to 6500 passes the coating wear rate and the coefficient of friction increased, but the ball wear rate decreased.

The coefficient of friction, the wear rate of the a-DLC top layer, and the ball wear rate were higher for silicon nitride sliding on a-DLC than for 440C stainless steel sliding on a-DLC. The wear life of the a-DLC top layer was slightly shorter when sliding against silicon nitride than when sliding against 440C stainless steel. When the a-DLC top layer was removed by sliding action and the Ti-Ti_xC_y underlayer was brought into contact with silicon nitride and with 440C stainless steel, the coefficient of friction and the wear rate of the Ti-Ti_xC_y underlayer increased. In this condition the wear rates of the silicon nitride and 440C stainless steel balls were almost the same.

Humid air environment.—In humid air with the materials pair of a-DLC/Ti-Ti_xC_y-DLC and 440C stainless steel ball, the a-DLC top layer was present in the entire wear track even at 550 000 sliding passes, providing a low coefficient of friction (0.11) and a low coating wear rate (on the order of 10^{-8} $mm^3/N•m$ or below). The wear rate of the 440C stainless steel ball was also extremely low (on the order of 10^{-10} $mm^3/N•m$).

Thus, the humid air environment provided a lower coefficient of friction, a lower wear rate of the a-DLC top layer, and a lower wear rate of the 440C stainless steel ball than occurred in the ultrahigh vacuum environment.

Sliding-Contact-Induced Transformation of a-DLC

Figure 16 presents Raman spectra of the as-deposited surface and the worn surface of the a-DLC/Ti-Ti_xC_y-DLC functionally gradient nanocomposite coating. The Raman spectrum of the worn surface (fig. 16(b)) was obtained from the wear track of the functionally gradient nanocomposite coating after 1000 sliding passes against a silicon nitride ball in ultrahigh vacuum. Changes in the bonding state and structure of the a-DLC layer were observed during the sliding friction process. The Raman spectrum of the as-deposited functionally gradient nanocomposite coating surface (fig. 16(a)) has the broad G-band with a peak near 1540 cm^{-1} indicative of the sp^2-bonded graphitic carbon. On the other hand, the Raman spectrum of the worn surface (fig. 16(b)) has a shoulder near 1340 cm^{-1} (D-band), indicative of the amorphous disordered nondiamond form of carbon, and a broad G-band (graphitic carbon) with a peak near 1550 cm^{-1}. Thus, the amorphous, disordered nondiamond form of carbon was formed during sliding contact.

CONCLUDING REMARKS

A marked difference in friction and wear of a-DLC/Ti-Ti_xCy-DLC functionally gradient nanocomposite coatings resulted from environmental conditions and combinations of materials. The humid air environment caused mild wear with burnishing in the a-DLC top layer, but the ultrahigh vacuum environment caused relatively severe wear with brittle fracture in both the a-DLC top layer and the Ti-Ti_xC_y-DLC underlayer. The humid air environment provided a preferable level of low coefficient of friction, low wear rate of the a-DLC top layer, and low ball wear rate of the 440C stainless steel (counterpart material).

In ultrahigh vacuum the levels of wear rate were acceptable for both the a-DLC coating and the 440C stainless steel ball. The materials pair of a-DLC top layer and 440C stainless steel ball was superior in wear resistance to the pair of a-DLC top layer and silicon nitride ball, although both the materials pairs had high coefficients of friction in ultrahigh vacuum.

Changes in the bonding state and structure of the a-DLC layer occurred during the sliding friction process. The amorphous, disordered nondiamond form of carbon was formed during sliding contact.

ACKNOWLEDGMENTS

The authors would like to thank Duane J. Dixon of Vehicle Technology Center for SEM; Rifka Cohen of the Kent State University for wear measurements; and Jerry Pobuda of Gilcrest for the experimental setups.

REFERENCES

1. Voevodin, A.A.; Walck, S.D.; and Zabinski, J.S.: Architectuíe of Multilayer Nanocomposite Coatings With Super-Hard Diamond-Like Carbon Layers for Wear Protection at High Contact Loads. Wear, vols. 203–204, 1997, pp. 516–527.
2. Holmberg, K.; and Ronkainen, H.: Coatings Tribology—Contact Mechanisms and Surface Design, in New Directions in Tribology. Mechanical Engineering Publications Limited for the Institute of Mechanical Engineers, London, 1997, pp. 251–267.
3. Fedoseev, D.V.; et al.: Multilayer Diamond-like Carbon Coatings. Diamond Relat. Mater., vol. 1, 1992, pp. 543–545.
4. Bentzon, M.D.; et al.: Metallic Interlayers Between Steel and Diamond-like Carbon. Surf. Coat. Technol., vols. 68–69, 1994, pp. 551–655.
5. Koskinen, J.; et al.: Characterization of the Mechanical Properties of Carbon Metal Multilayered Films. Diamond Relat. Mater., vol. 4, 1995, pp. 843–847.
6. Kupfer, H.; et al.: Deposition and Properties of TiN/Carbon Multilayers for Corrosion Protection of Steels. Surf. Coat. Technol., vols. 74–75, 1995, pp. 333–338.
7. Li, D.; et al.: Structure and Hardness Studies of CN_x/TiN Nanocomposite Coatings. Appl. Phys. Lett., vol. 68, 1996, pp. 1211–1213.
8. Miyoshi, K.; Wu, R.L.C.; and Lanter, W.C.: Friction and Wear of Diamondlike Carbon on Fine-Grain Diamond. Tribol. Lett., vol. 3, 1997, pp. 141–145.
9. Voevodin, A.A.; et al.: Mechanical and Tribological Properties of Diamond-like Coatings Prepared by Pulsed Laser Deposition. Surf. Coat. Technol., vols. 76–77, 1995, pp. 534–539.
10. Dimigen, H.; and Klages, C.-P.: Microstructure and Wear Behavior of Metal-Containing Diamond-like Coatings. Surf. Coat. Technol., vol. 49, 1993, pp. 543–547.
11. Voevodin, A.A.; Bantle, R.; and Matthews, A.: Dynamic Impact Wear of TiC_xN_y and Ti-DLC Composite Coatings. Wear, vol. 185, 1995, pp. 151–157.
12. Voevodin, A.A.; Rebholz, C.; and Matthews, A.: Comparative Tribology Studies of Hard Ceramic and Composite Metal-DLC Coatings in Sliding Friction Conditions. STLE J. Tribol. Trans., vol. 38, 1995, pp. 829–836.
13. Wu, R.L.C.; et al.: Physical and Tribological Properties of Rapid Thermal Annealed Diamond-like Carbon Films. Surf. Coat. Technol., vols. 54–55, 1992, pp. 576–580.

14. Miyoshi, K.; Pouch, J.J.; and Alterovitz, S.A.: Plasma-Deposited Amorphous Hydrogenated Carbon Films and Their Tribological Properties. Materials Science Forum, vols. 52–53, Trans Tech Publications, Aedermannsdorf, Switzerland, 1989, pp. 645–656.
15. Voevodin, A.A.; et al.: Design of a Ti/TiC/DLC Functionally Gradient Coating Based on Studies of Structural Transitions in Ti-C Films. Thin Solid Films, vol. 298, 1997, pp. 107–115.
16. Voevodin, A.A.; et al.: Combined Magnetron Sputtering and Pulsed Laser Deposition of Carbides and Diamond-like Carbon Films. Appl. Phys. Lett., vol. 69, no. 2, 1996, pp. 188–190.
17. Wu, R.L.C.; et al.: Uniform and Large Area Deposition of Diamond-like Carbon Using RF Source Ion Beam. Mater. Res. Soc. Symp. Proc., vol. 354, 1995, p. 63.

TABLE I.—TRIBOLOGICAL PROPERTIES FOR MULTILAYER COATING–SILICON NITRIDE BALL PAIR AND –440C STAINLESS STEEL BALL PAIR IN ULTRAHIGH VACUUM OR HUMID AIR

(a) Counterpart ball specimen, silicon nitride

Environment	Status of a-DLC in wear track	Average steady-state coefficient of friction	Average wear rate of coating, $mm^3/N\text{-}m$	Average wear rate of ball, $mm^3/N\text{-}m$
Ultrahigh vacuum	Present to 800 to 900 passes	0.60	9.1×10^{-6}	1.8×10^{-6}
	Delaminated locally at center of wear track to 4000 to 5000 passes	0.56	3.7×10^{-6}	1.7×10^{-6}
	Absent above 5000 passes	0.86	5.2×10^{-5}	7.9×10^{-7}

(b) Counterpart ball specimen, 440C stainless steel

Ultrahigh vacuum	Present to 1100 to 1200 passes	0.56	4.2×10^{-6}	1.5×10^{-7}
	Delaminated locally at center of wear track to 4400 to 6500 passes	0.70	9.9×10^{-6}	2.6×10^{-7}
	Absent above 6500 passes	0.92	3.0×10^{-5}	7.7×10^{-7}
Humid air	Present even at 550 000 passes	0.11	1.3×10^{-8}	8.1×10^{-10}

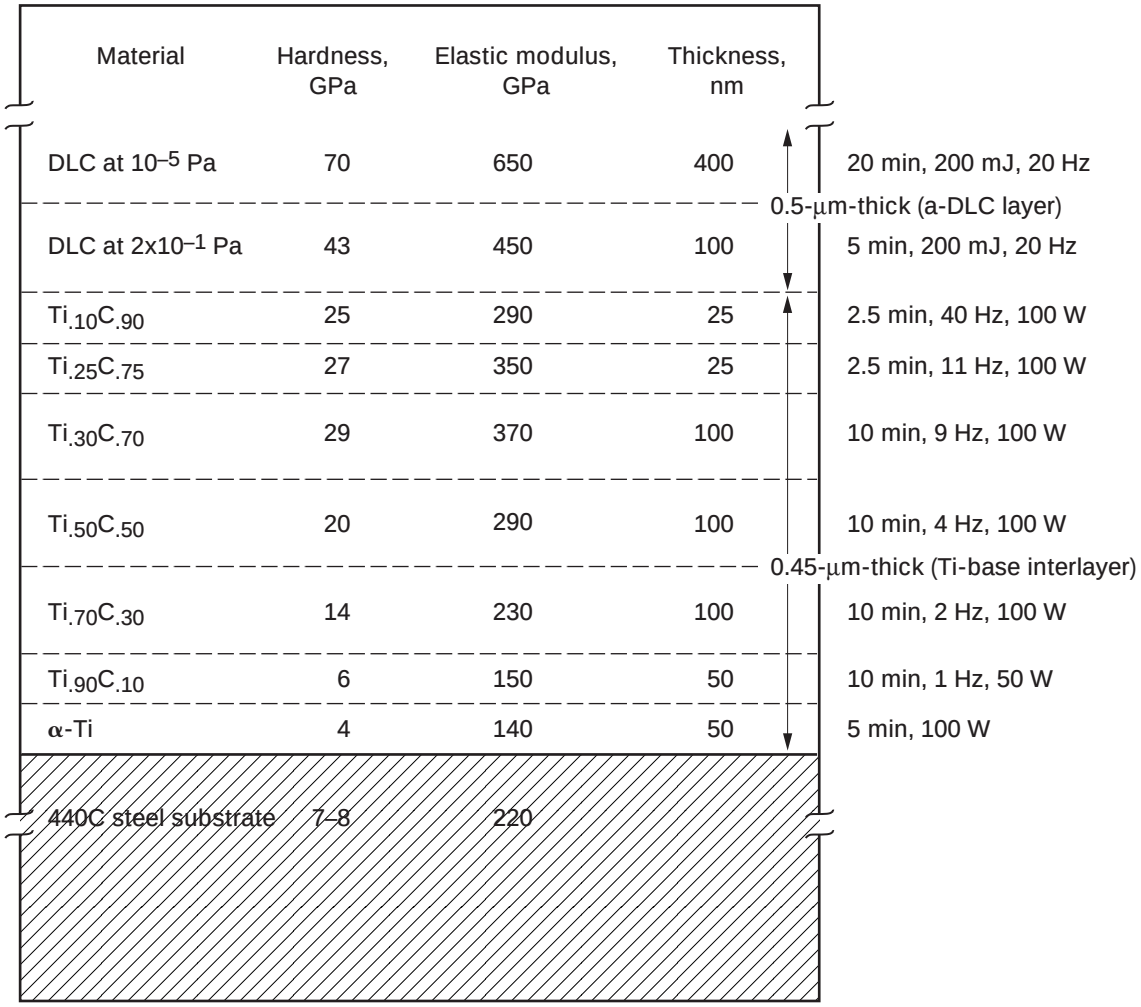

Figure 1.—Schematic diagram of functionally gradient a-DLC/Ti-Ti_xC_y-DLC multilayer coating showing gradation of composition and hardness across coating thickness.

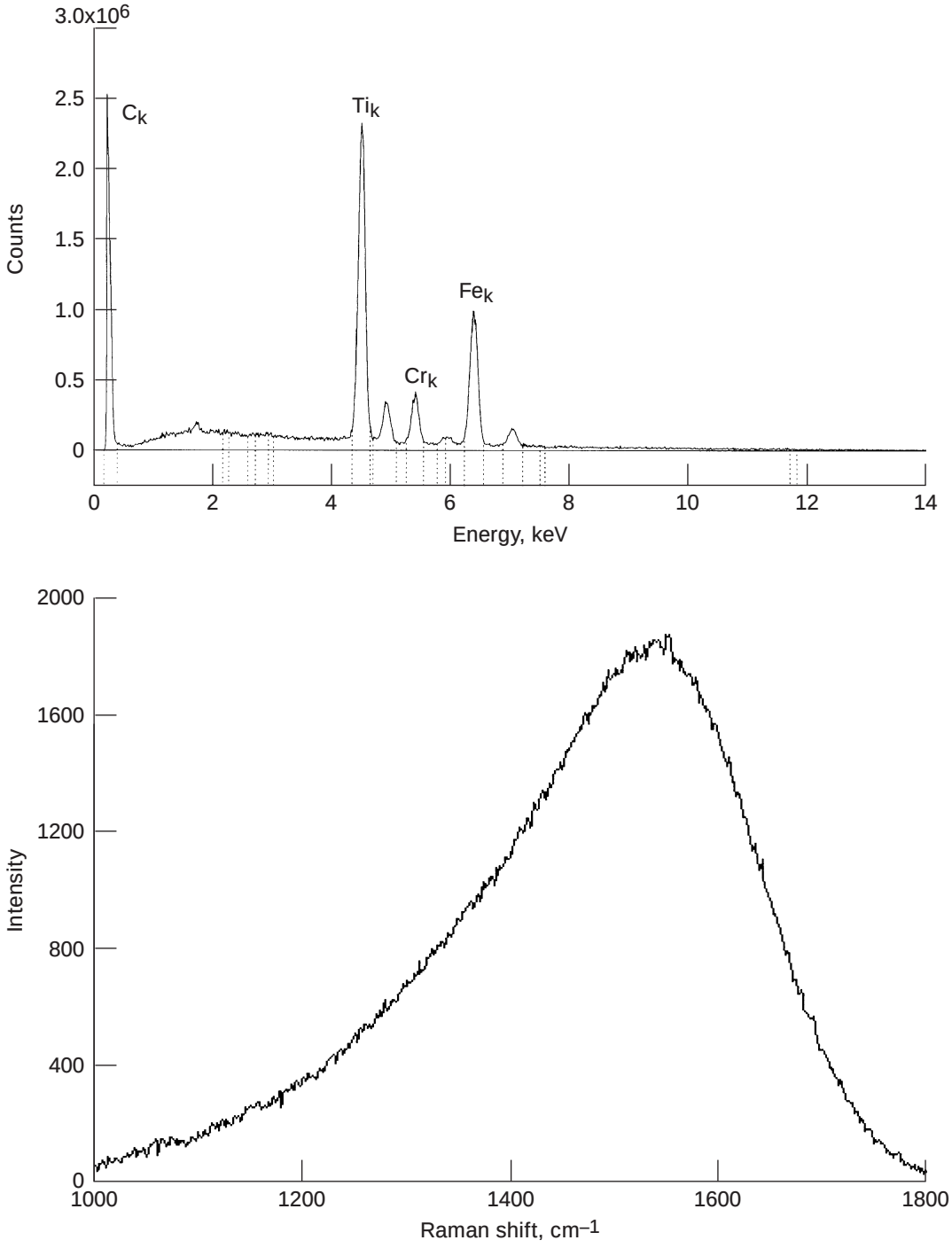

Figure 2.—EDX and Raman spectra of a-DLC/Ti-Ti_xC_y-DLC multilayer coating.

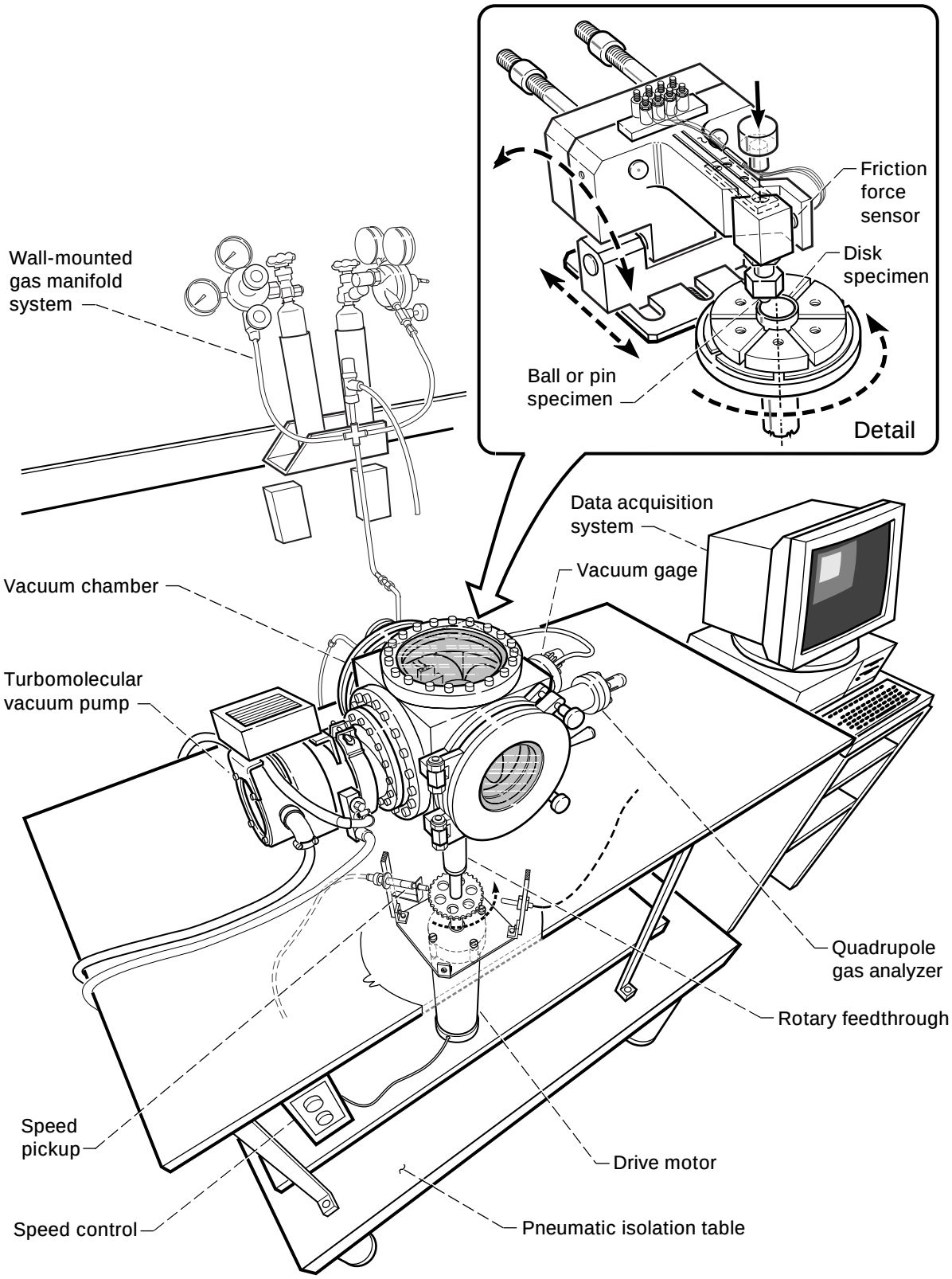

Figure 3.—Vacuum chamber friction-and-wear apparatus.

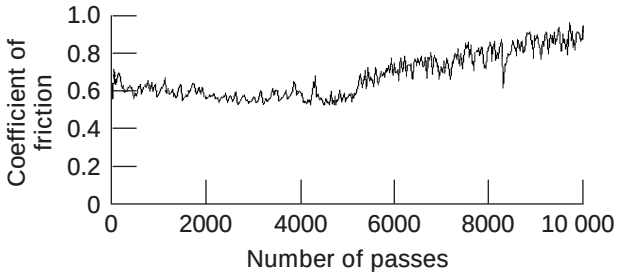

Figure 4.—Friction trace for a-DLC/Ti-Ti_xC_y-DLC multilayer coating in sliding contact with silicon nitride ball as function of number of passes in ultrahigh vacuum.

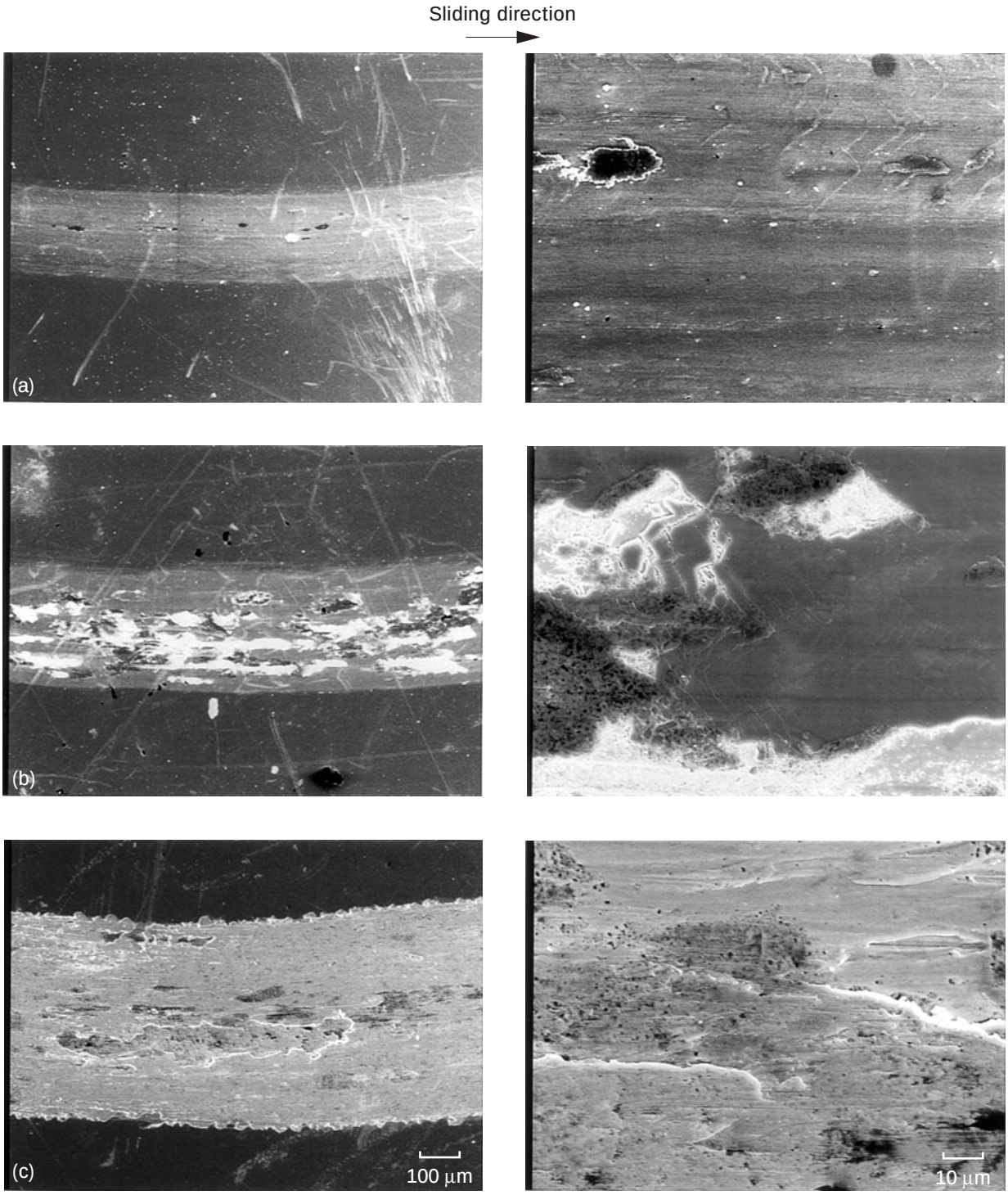

Figure 5.—SEM photomicrographs of worn surfaces of a-DLC/Ti-Ti_xC_y-DLC multilayer coatings after sliding contact with silicon nitride balls in ultrahigh vacuum. (Right photograph of each part is a higher magnification.) (a) After 300 passes. (b) After 1000 passes. (c) After 10 000 passes.

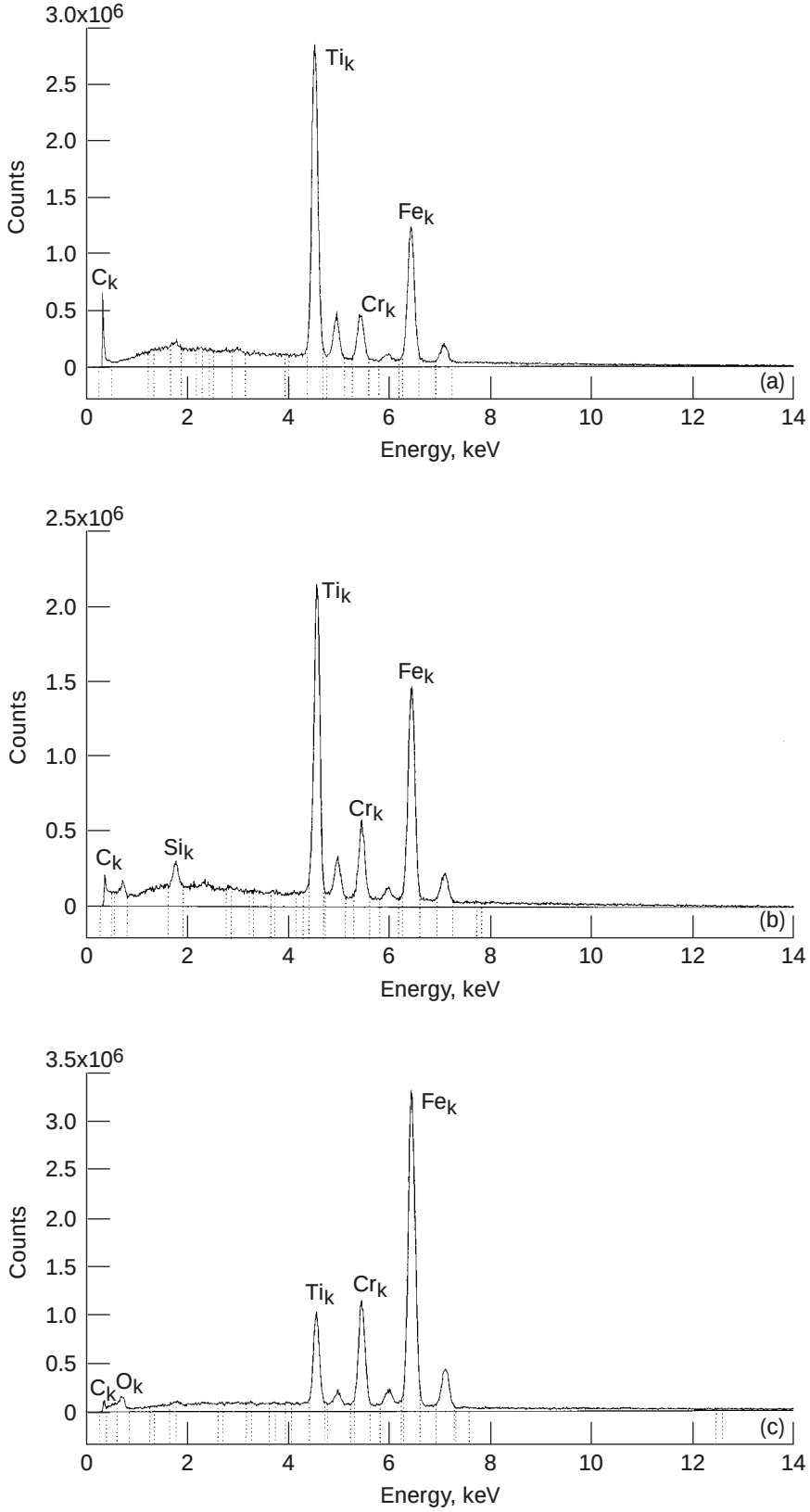

Figure 6.—EDX spectra of worn surfaces of a-DLC/Ti-Ti_xC_y-DLC multilayer coatings after sliding contact with silicon nitride balls in ultrahigh vacuum. (a) After 300 passes. (b) After 1000 passes. (c) After 10 000 passes.

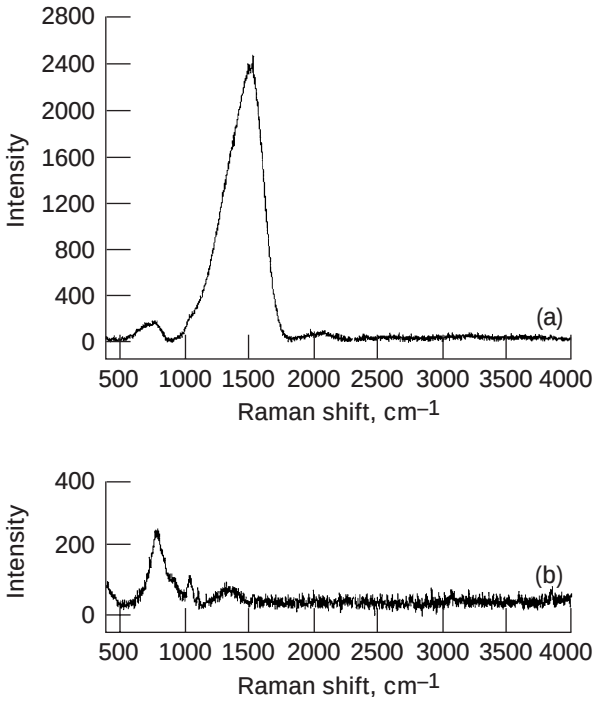

Figure 7.—Raman spectra of a-DLC/Ti-Ti_xC_y-DLC multilayer coating before and after 10 000 sliding passes against silicon nitride ball in ultrahigh vacuum. (a) As-deposited surface. (b) Worn surface.

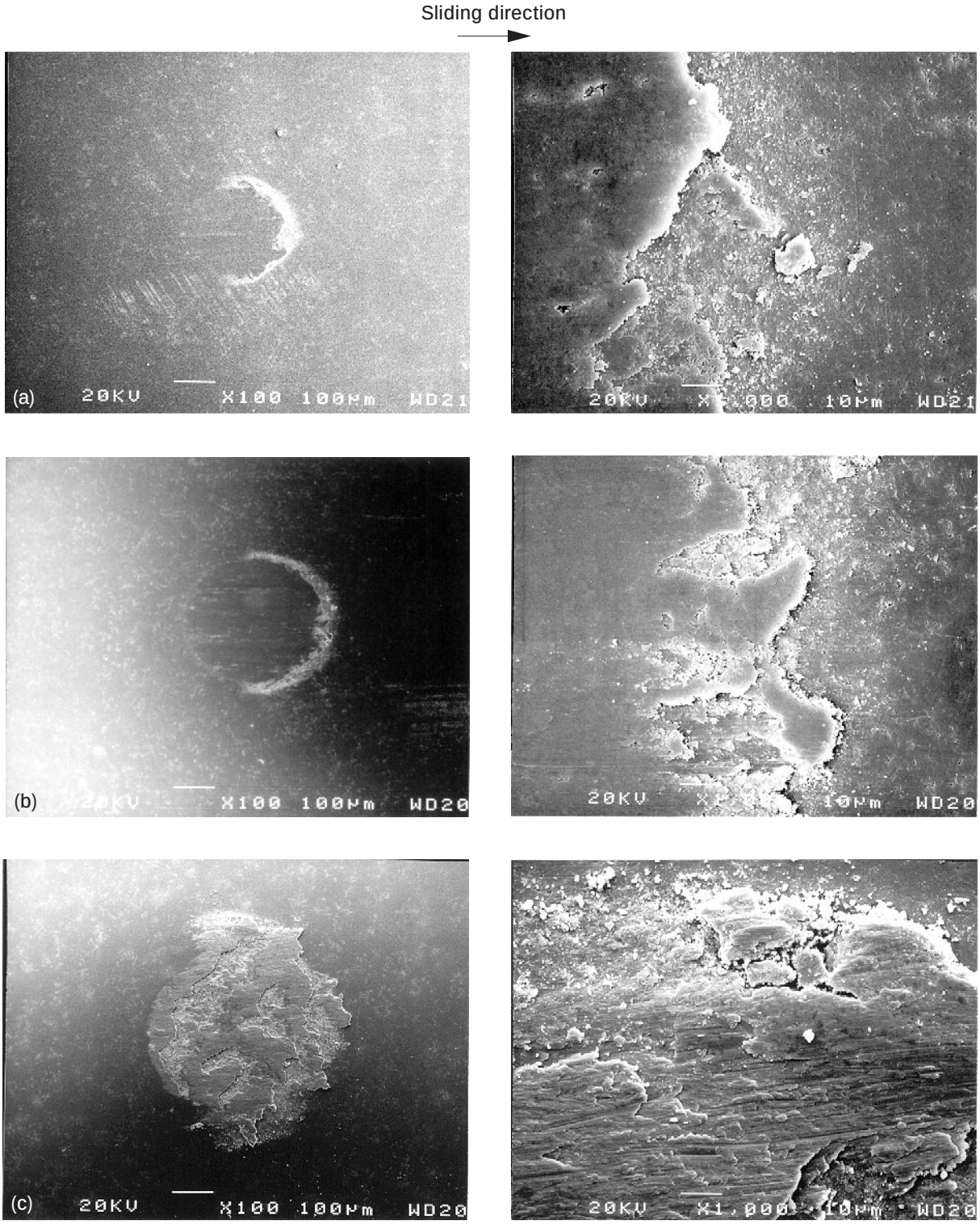

Figure 8.—SEM photomicrographs of wear scars on silicon nitride balls after sliding against a-DLC/Ti-Ti_xC_y-DLC multilayer coatings in ultrahigh vacuum. (First photograph of each part is a general view; second shows the location of wear debris; third shows the center of the wear scar.) (a) After 300 passes. (b) After 1000 passes. (c) After 10 000 passes.

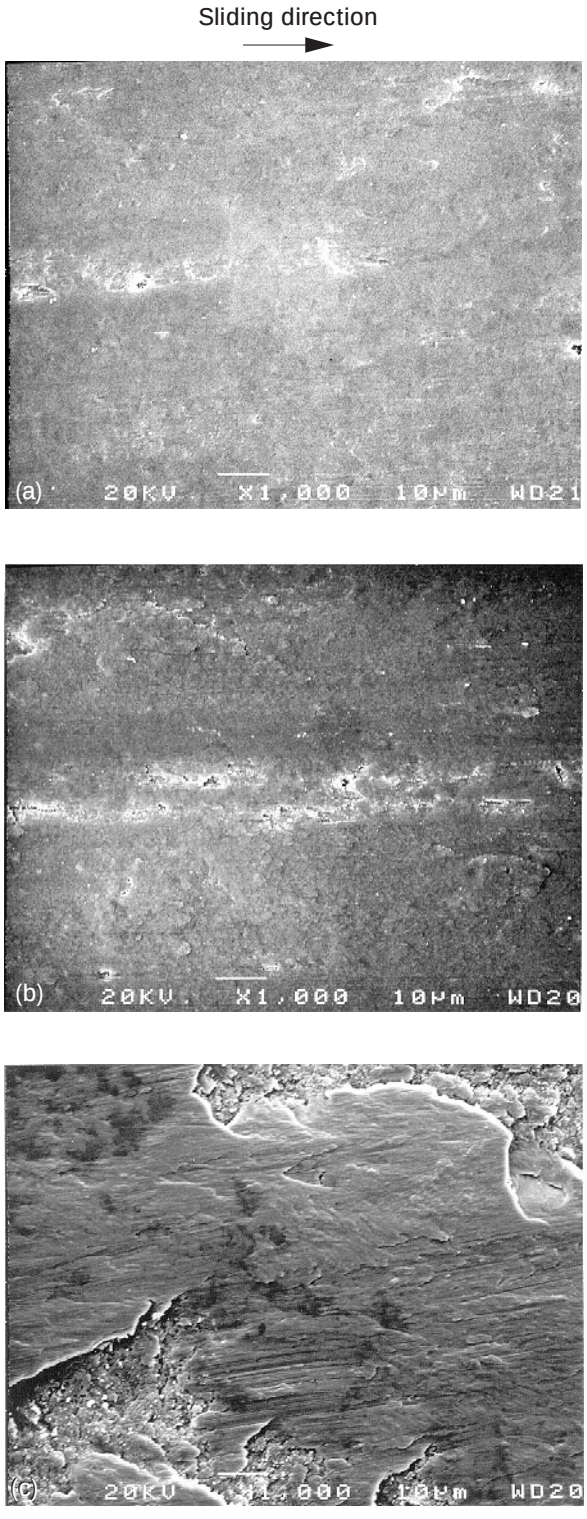

Figure 8.—Concluded. (a) After 300 passes. (b) After 1000 passes. (c) After 10 000 passes.

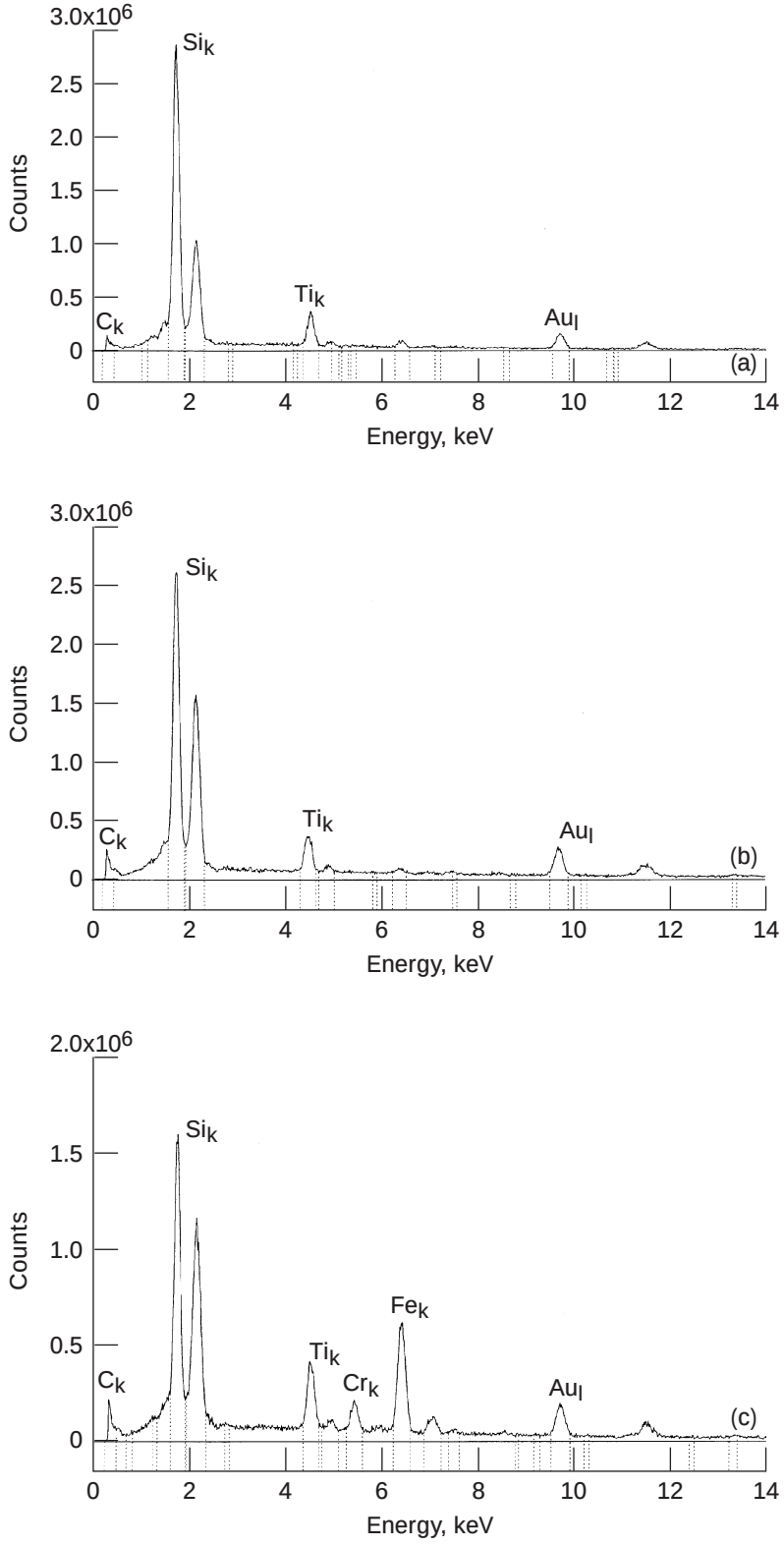

Figure 9.—EDX spectra of center of wear scars on silicon nitride balls after sliding against a-DLC/Ti-Ti_xC_y-DLC multilayer coatings in ultrahigh vacuum. (a) After 300 passes. (b) After 1000 passes. (c) After 10 000 passes. The thin gold film used to reduce charging of the balls is responsible for the gold signal in the three spectra.

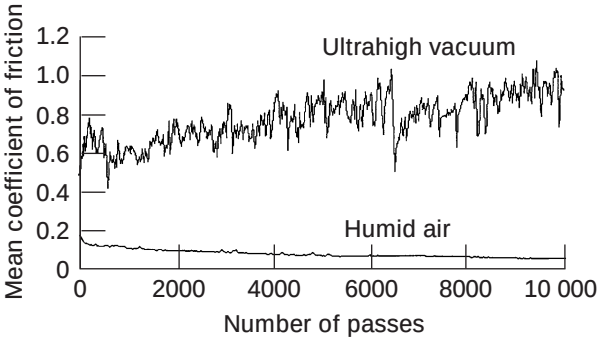

Figure 10.—Typical friction traces for a-DLC/Ti-Ti_xC_y-DLC multilayer coatings in sliding contact with 440C stainless steel balls as function of number of passes in ultrahigh vacuum and in humid air.

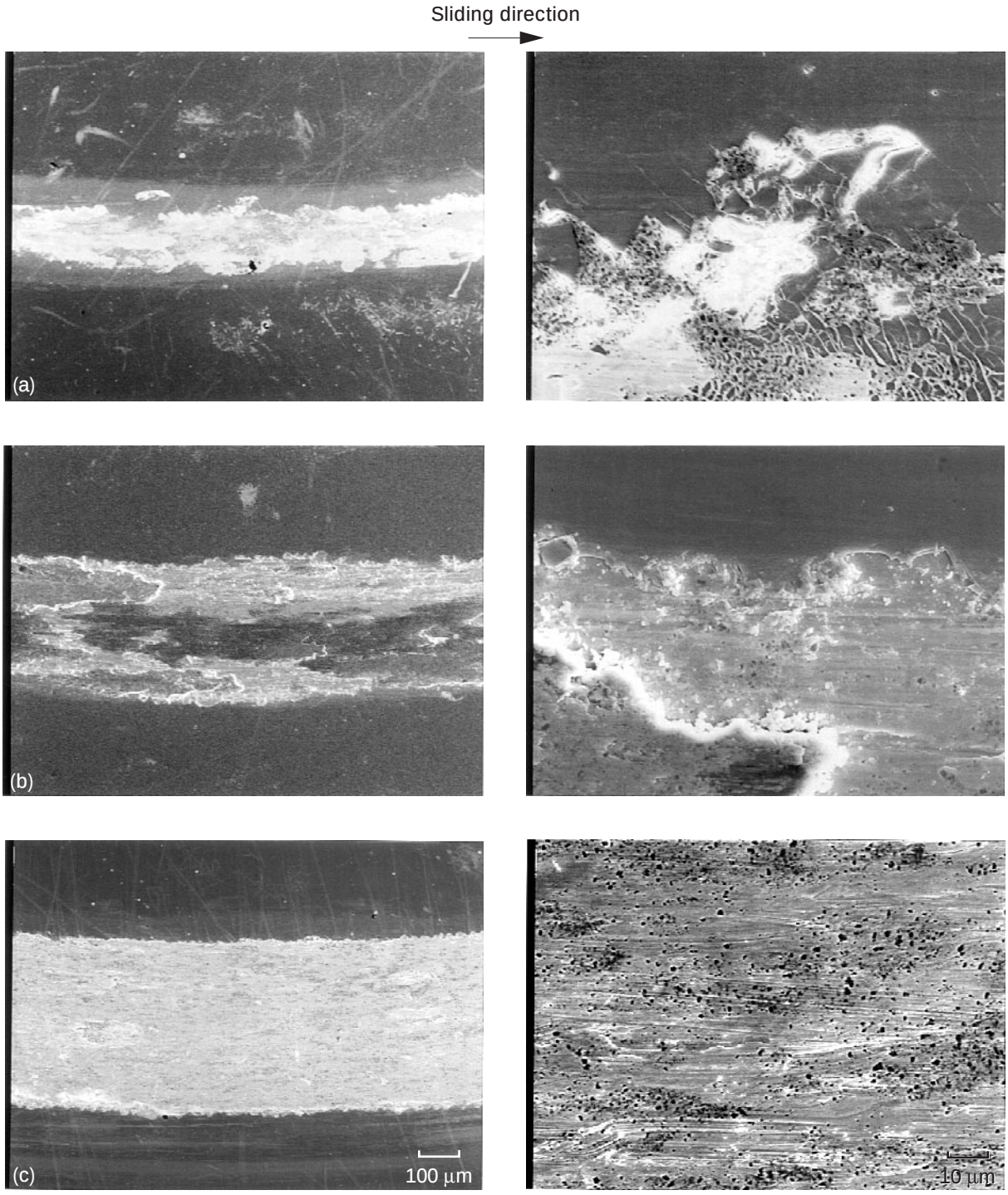

Figure 11.—SEM photomicrographs of worn surfaces of a-DLC/Ti-Ti_xC_y-DLC multilayer coatings after sliding contact with 440C stainless steel balls in ultrahigh vacuum. (Right photograph of each part is a higher magnification.) (a) After 3000 passes. (b) After 6000 passes. (c) After 10 000 passes.

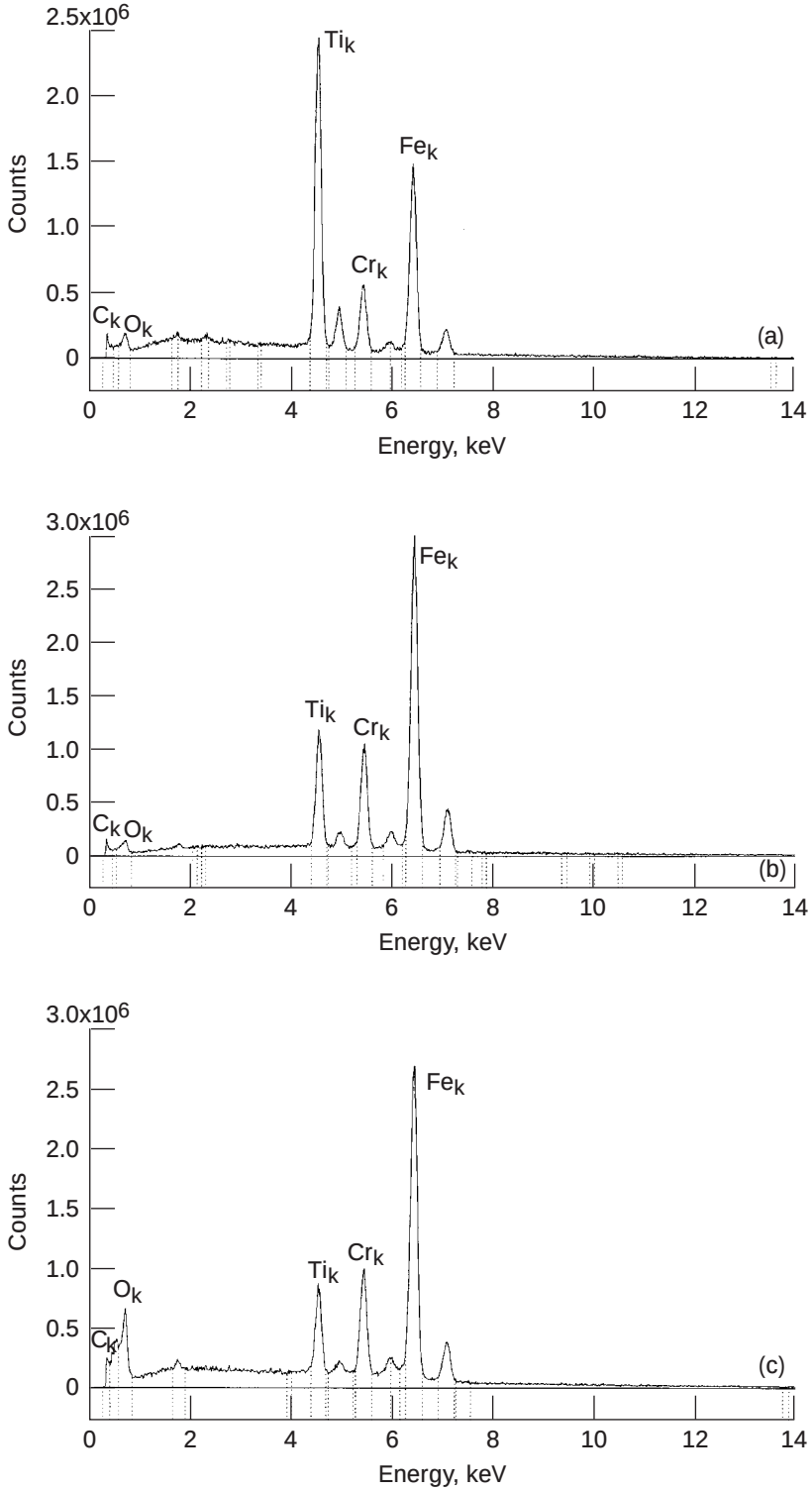

Figure 12.—EDX spectra of worn surfaces of a-DLC/Ti-Ti_xC_y-DLC multilayer coatings after sliding contact with 440C stainless steel balls in ultrahigh vacuum. (a) After 3000 passes. (b) After 6000 passes. (c) After 10 000 passes.

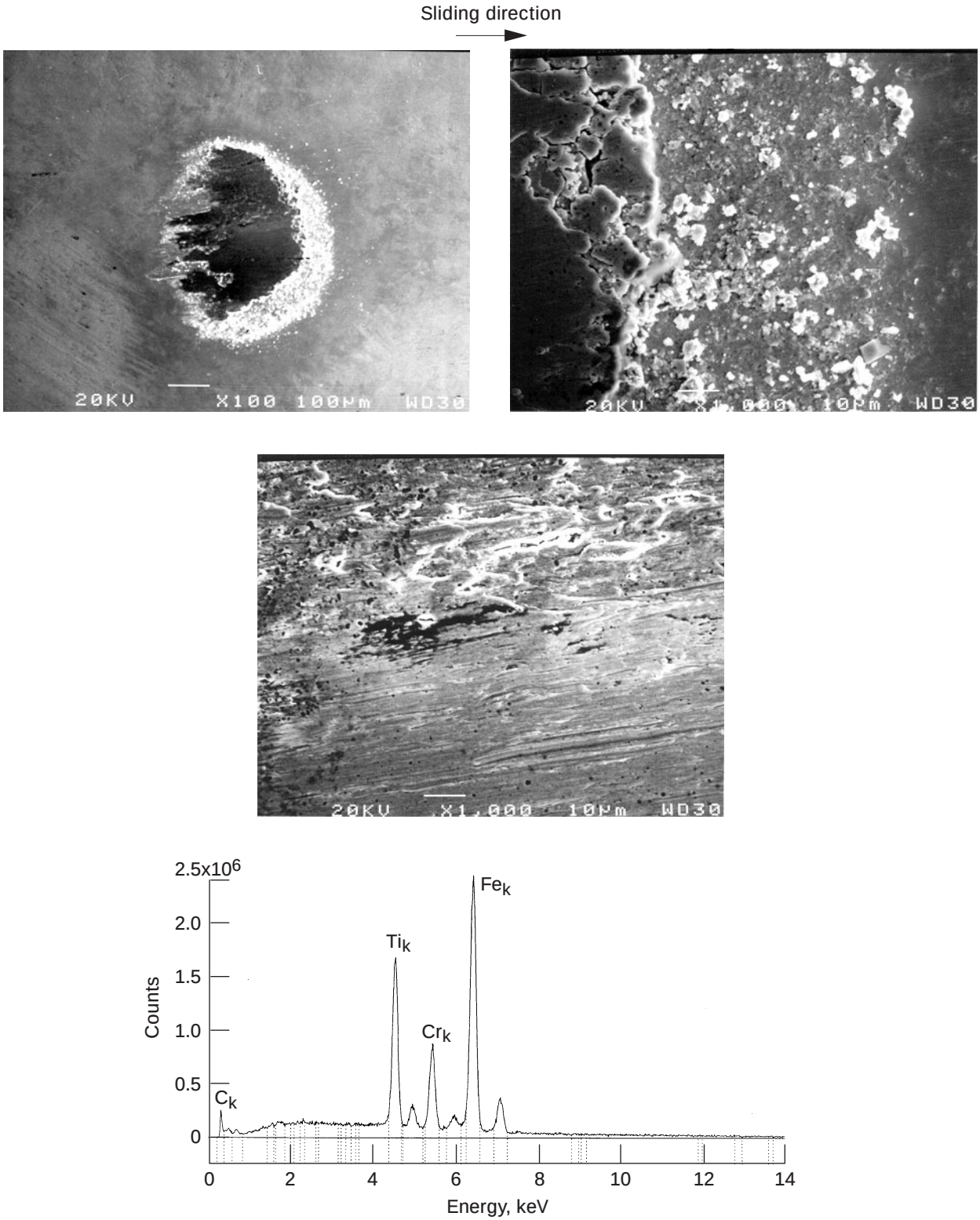

Figure 13.—SEM photomicrographs and EDX spectrum of wear scar on 440C stainless steel ball after 10 000 sliding passes against a-DLC/Ti-Ti_xC_y-DLC multilayer coating in ultrahigh vacuum.

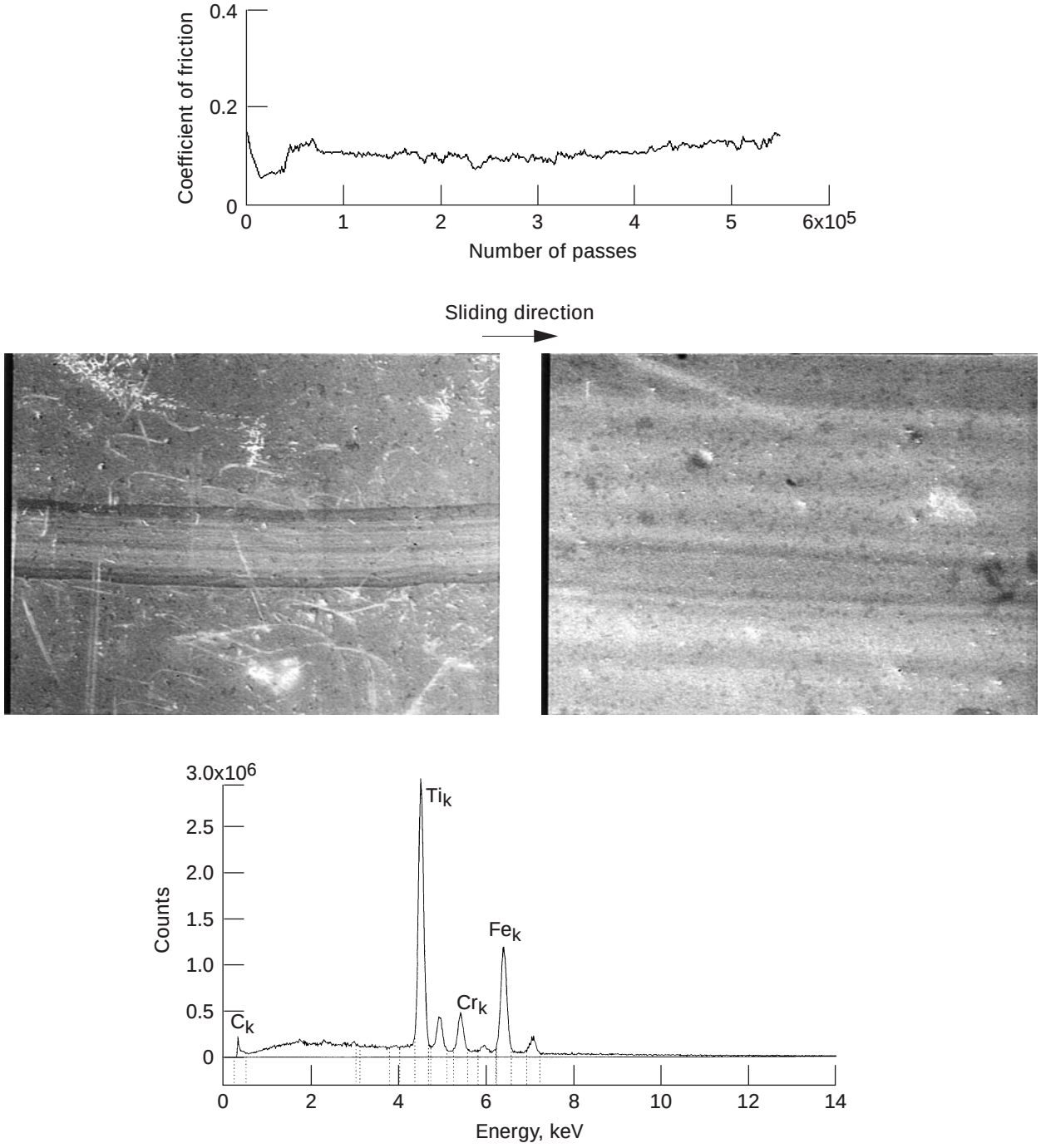

Figure 14.—Friction trace, SEM photomicrographs, and EDX spectrum for a-DLC/Ti-Ti_xC_y-DLC multilayer coating in sliding contact with 440C stainless steel ball to 550 000 passes in humid air.

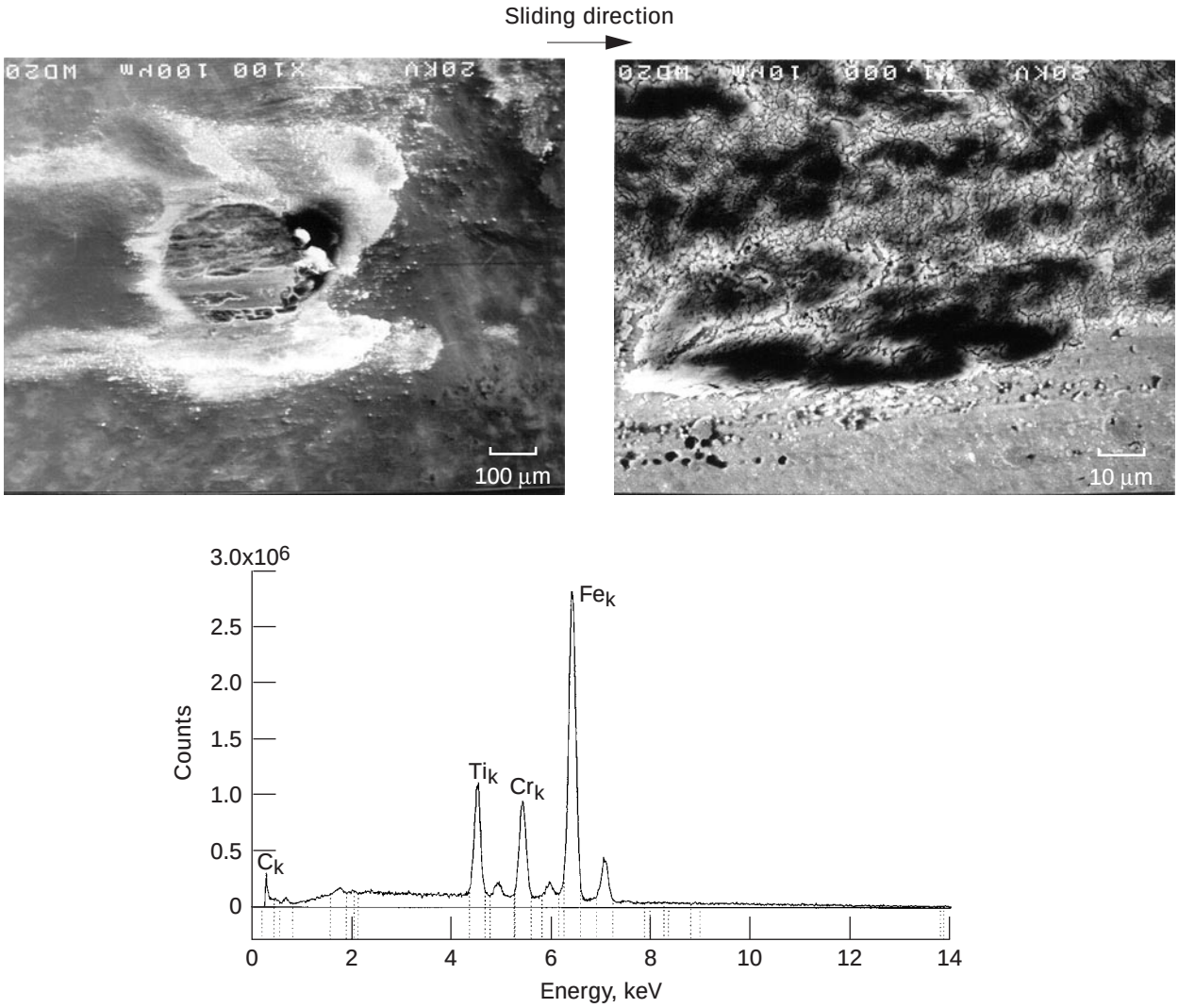

Figure 15.—SEM photomicrographs and EDX spectrum of wear scar on 440C stainless steel ball after 550 000 sliding passes against a-DLC/Ti-Ti_xC_y-DLC multilayer coating in humid air.

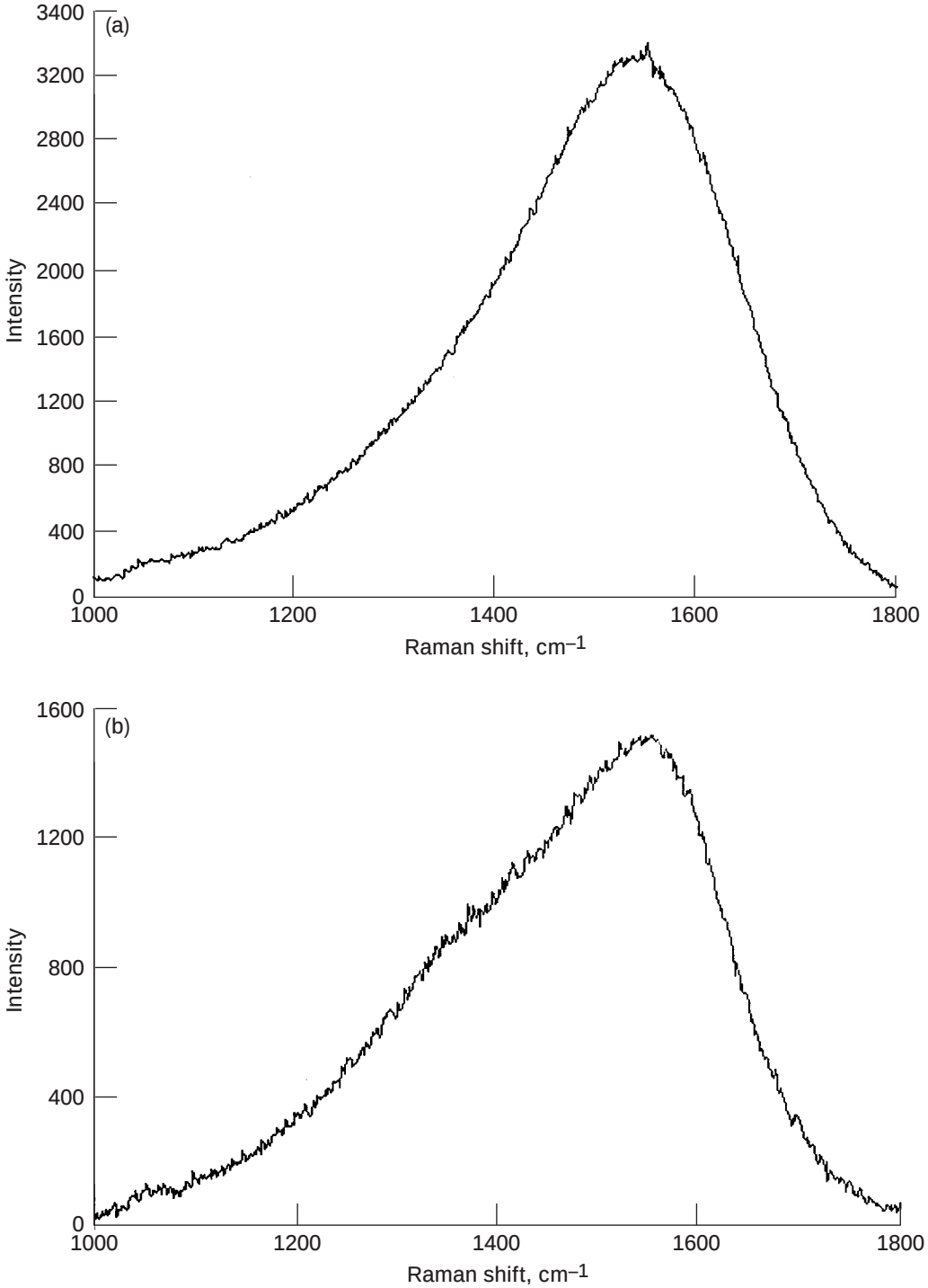

Figure 16.—Raman spectra of a-DLC/Ti-Ti_xC_y-DLC multilayer coating before and after 1000 sliding passes against silicon nitride ball in ultrahigh vacuum. (a) As-deposited surface. (b) Worn surface.

REPORT DOCUMENTATION PAGE

Form Approved
OMB No. 0704-0188

1. AGENCY USE ONLY (*Leave blank*)	2. REPORT DATE	3. REPORT TYPE AND DATES COVERED
	March 1998	Technical Memorandum

4. TITLE AND SUBTITLE

Friction and Wear Properties of a-DLC-Based Functionally Gradient Nanocomposite Coatings

5. FUNDING NUMBERS

WU–523–22–13–00

6. AUTHOR(S)

Kazuhisa Miyoshi, Kenneth W. Street, Jeffrey S. Zabinski, Jeffrey H. Sanders, and Andrey A. Voevodin

7. PERFORMING ORGANIZATION NAME(S) AND ADDRESS(ES)

National Aeronautics and Space Administration
Lewis Research Center
Cleveland, Ohio 44135–3191

8. PERFORMING ORGANIZATION REPORT NUMBER

E–10972

9. SPONSORING/MONITORING AGENCY NAME(S) AND ADDRESS(ES)

National Aeronautics and Space Administration
Washington, DC 20546–0001

10. SPONSORING/MONITORING AGENCY REPORT NUMBER

NASA TM—1998-206962

11. SUPPLEMENTARY NOTES

Kazuhisa Miyoshi and Kenneth W. Street, NASA Lewis Research Center; Jeffrey S. Zabinski, Jeffrey H. Sanders, and Andrey A. Voevodin, Air Force Research Laboratory, Wright-Patterson Air Force Base, Ohio 45433–7750. Responsible person, Kazuhisa Miyoshi, organization code 5140, (216) 433–6078.

12a. DISTRIBUTION/AVAILABILITY STATEMENT

Unclassified - Unlimited
Subject Category: 27 Distribution: Nonstandard

This publication is available from the NASA Center for AeroSpace Information, (301) 621–0390.

12b. DISTRIBUTION CODE

13. ABSTRACT ***(Maximum 200 words)***

An investigation was conducted to examine the friction and wear behavior of an amorphous diamondlike carbon (a-DLC or a-C) functionally gradient nanocomposite coating in sliding contact with a 6-mm-diameter silicon nitride ball and a 6-mm-diameter 440C stainless steel ball in ultrahigh vacuum and in humid air. The nanocomposite coatings, consisting of an a-DLC top layer and a gradient Ti-Ti_xC_y-DLC underlayer, were produced by the hybrid technique of magnetron sputtering and pulsed-laser deposition on 440C stainless steel substrates.The resultant coatings were characterized by Raman spectroscopy, scanning electron microscopy, energy-dispersive x-ray spectroscopy, and surface profilometry. All sliding friction experiments were conducted with a load of 0.98 N (100 g), average Hertzian contact pressures of 0.6 GPa with the 440C stainless steel balls and 0.8 GPa with the silicon nitride balls, and 120 revolutions per minute. The sliding velocity ranged from 31 to 107 mm/s because of the range of wear track radii involved in the experiments. The experiment was conducted at room temp-erature in two environments: ultrahigh vacuum (vacuum pressure, 7×10^{-7} to 2×10^{-6} Pa) and humid air (relative humidity, about 50%).A marked difference in friction and wear resulted from the environmental conditions and the combination of materials. The humid air caused mild wear with burnishing in the a-DLC top layer; the ultrahigh vacuum caused relatively severe wear with brittle fracture in both the a-DLC top layer and the Ti-Ti_xC_y-DLC underlayer. The humid air environment provided a low coefficient of friction, a low wear rate for the a-DLC top layer, and a low wear rate for the 440C stainless steel ball (counterpart material). In ultrahigh vacuum the materials pair of a-DLC coated substrate and 440C stainless steel ball was superior in wear resistance to the pair of a-DLC and silicon nitride ball, although both pairs had high coefficients of friction. The wear rate was low in both environments for both the a-DLC coated substrate and the 440C stainless steel ball. Changes in the bonding state and structure of the a-DLC layer were observed during the sliding friction process. The amorphous, disordered nondiamond form of carbon was produced during sliding contact.

14. SUBJECT TERMS	15. NUMBER OF PAGES
Friction; Wear; a-DLC coating	30
	16. PRICE CODE: A03

17. SECURITY CLASSIFICATION OF REPORT	18. SECURITY CLASSIFICATION OF THIS PAGE	19. SECURITY CLASSIFICATION OF ABSTRACT	20. LIMITATION OF ABSTRACT
Unclassified	Unclassified	Unclassified	